

Ultra high energy cosmic rays from extragalactic astrophysical sources: energy losses and spectra

V. Berezhinsky^{1,3}, A.Z. Gazizov² and S.I. Grigorieva³

¹*INFN, Laboratori Nazionali del Gran Sasso, I-67010 Assergi (AQ), Italy,*

²*B. I. Stepanov Institute of Physics of the National Academy of Sciences of Belarus,*

F. Skariny Ave. 68, 220062 Minsk, Belarus

³*Institute for Nuclear Research of Russian Academy of Sciences,*

60th Anniversary of October Revolution prospect 7A, 117312 Moscow, Russia

Abstract

The energy losses and spectra of Ultra High Energy Cosmic Rays (UHECR) are calculated for protons as primary particles. The attention is given to the energy losses due to electron-positron production in collisions with the microwave 2.73 K photons. The energy spectra are calculated for several models, which differ by production spectra and by source distribution, namely:

- (i) Uniform distribution of the sources with steep generation spectra with indices 2.4 - 2.7, with cosmological evolution and without it. In this case it is possible to fit the shape of the observed spectrum up to $8 \cdot 10^{19}$ eV, but the required CR emissivity is too high and the GZK cutoff is present.
- (ii) Uniform distribution of the sources with flat generation spectrum dE/E^2 which is relevant to GRBs. The calculated spectrum is in disagreement with the observed one. The agreement at $E \lesssim 8 \cdot 10^{19}$ eV can be reached using a complex generation spectrum, but the required CR emissivity is three orders of magnitude higher than that of GRBs, and the predicted spectrum has the

GZK cutoff. *(iii)* The case of local enhancement within region of size 10 - 30 Mpc with overdensity given by factor 3 - 30. The overdensity larger than 10 is needed to eliminate the GZK cutoff.

I. INTRODUCTION

The energy losses of UHE protons in extragalactic space are caused by interaction with microwave radiation. The contribution of IR and optical radiation is small (for a detailed review of energy losses and the resulting spectrum see [1]). The main contribution to energy losses is given by expansion of the universe, electron-positron pair production and pion production. The latter process results in steepening of the proton spectrum referred to as the Greisen-Zatsepin-Kuzmin (GZK) cutoff [2]. The GZK cutoff is not seen in the observational data (for a recent review see [3]). The most conservative approach to explanation of observations is astrophysical one: the protons are accelerated in extragalactic astrophysical sources (normal galaxies, compact objects in normal galaxies, e.g. GRB engines, AGN etc) and propagate towards us. This approach comprises three aspects: acceleration to UHE, total energy release in a source and propagation in extragalactic space. This most conservative approach is considered as (almost) excluded, with certain caveats, however. The models in which the GZK cutoff is absent or ameliorated include nearby *one-source model* (see [4,5] and most recent work [6]); the *Local Supercluster model*, in which the density of UHECR sources is locally enhanced ([1,7], for a recent work see [8]); and finally widely discussed *GRB model* which, according to calculations [9], gives a reasonable agreement with observations.

In this paper we shall analyse the two latter models.

II. ENERGY LOSSES

We present here the accurate calculations for pair production, $p + \gamma_{CMBR} \rightarrow p + e^+ + e^-$, and for pion production $p + \gamma_{CMBR} \rightarrow N + \text{pions}$, where γ_{CMBR} is a microwave photon.

The energy losses of UHE proton per unit time due to its interaction with low energy photons is given by

$$-\frac{1}{E} \frac{dE}{dt} = \frac{c}{2\Gamma^2} \int_{\epsilon_{th}}^{\infty} d\epsilon_r \sigma(\epsilon_r) f(\epsilon_r) \epsilon_r \int_{\epsilon_r/2\Gamma}^{\infty} d\epsilon \frac{n(\epsilon)}{\epsilon^2}, \quad (1)$$

where Γ is the Lorentz factor of the proton, ϵ_r is the energy of background photon in the system where the proton is at rest, ϵ_{th} is the threshold of the considered reaction in the rest system of the proton, $\sigma(\epsilon_r)$ is the cross-section, $f(\epsilon_r)$ is the mean fraction of energy lost by the proton in one $p\gamma$ collision in the laboratory system, ϵ is the energy of the background photon in the lab system, and $n(\epsilon)$ is the density of background photons.

For the CMBR with temperature T Eq.(1) is simplified

$$-\frac{1}{E} \frac{dE}{dt} = \frac{cT}{2\pi^2\Gamma^2} \int_{\epsilon_{th}}^{\infty} d\epsilon_r \sigma(\epsilon_r) f(\epsilon_r) \epsilon_r \left\{ -\ln \left[1 - \exp \left(-\frac{\epsilon_r}{2\Gamma T} \right) \right] \right\}. \quad (2)$$

From Eqs.(1) and (2) one can see that the mean fraction of energy lost by the proton in lab system in one collision, $f(\epsilon_r) = \langle 1 - x \rangle = (E_p - E'_p)/E_p$, is the basic quantity needed for calculations of energy losses. The threshold values of these quantities are well known:

$$f_{\text{pair}} \approx \frac{2m_e}{m_p}, \quad f_{\text{pion}} \approx \frac{\epsilon_r}{m_p} \frac{1 + \mu^2/2\epsilon_r m_p}{1 + 2\epsilon_r/m_p}, \quad (3)$$

where f_{pair} and f_{pion} are the threshold fractions for $p + \gamma \rightarrow p + e^+ + e^-$ and $p + \gamma \rightarrow N + \pi$, respectively, and μ is the pion mass.

For the accurate calculations of energy losses the fraction f properly averaged over differential cross-section is needed.

Pair production loss has been previously discussed in many papers. All authors directly or indirectly have followed the standard approach of Ref. [10] where the first Born approximation of the Bethe-Heitler cross-section with proton mass $m_p \rightarrow \infty$ was used. In contrast to

Ref. [10], we are using the first Born approximation approach of Ref. [11], which takes into account the finite proton mass. We also use the exact non-relativistic differential cross-section from [12]. This allowed us to calculate the average fraction of energy lost by the proton in lab system by performing fourfold integration over invariant mass of electron-positron pair M_X , over an angle between incident and scattered proton, and polar and azimuthal angles of an electron in the c.m system of the pair (see Appendix A for further details).

Calculating photopion energy loss we followed the method of papers [13,14]. Total cross-sections were taken according to Ref. [15]. At low c.m. energy E_c we considered the binary reactions $p + \gamma \rightarrow \pi + N$ (including the resonance $p + \gamma \rightarrow \Delta$), $p + \gamma \rightarrow \pi^- + \Delta^{++}$, and $p + \gamma \rightarrow \rho^0 + p$. Differential cross-sections of binary processes at small energies were taken from [16]. At $E_c > 4.3$ GeV we assumed the scaling behaviour of differential cross-sections. These were taken from Ref. [17]. In the intermediate energy range we used an interpolation approach which allows us to describe the residual part of the total cross-section. The corresponding differential cross-sections coincide with low-energy binary description and high-energy scaling distribution and have a smooth transition between these two regimes in the intermediate region.

FIGURES

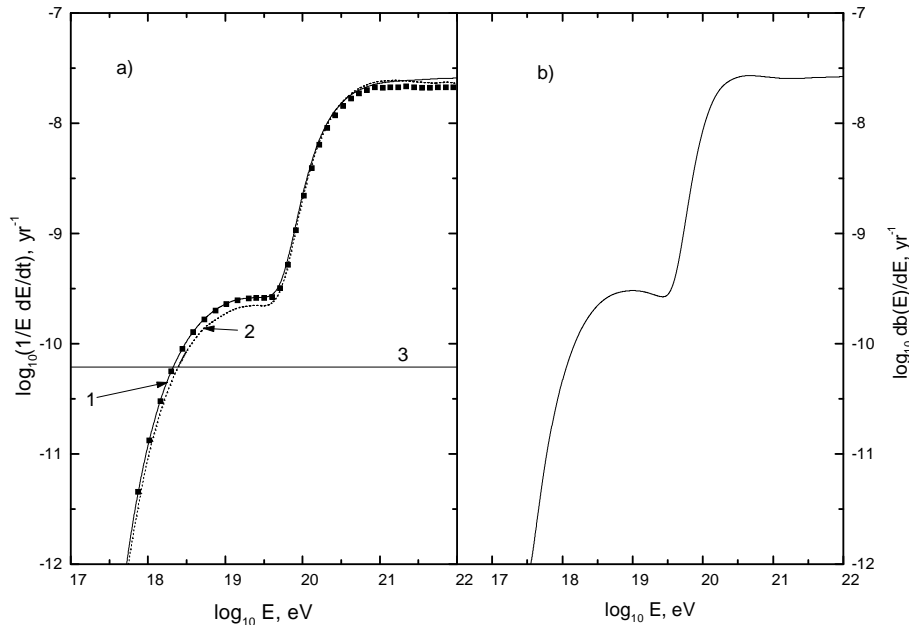


FIG. 1. a) *UHE proton energy losses* $E^{-1}dE/dt$ (present work: curve 1; Berezinsky and Grigorieva (1988) [19]: curve 2; Stanev et al 2000 [18] : black squares). The line 3 gives energy losses due to redshift ($H_0 = 65$ km/sMpc). b) The derivative $db_0(E)/dE$, where $b_0(E) = dE/dt$ at present epoch $z = 0$.

The results of our calculations are presented in Fig.1 in terms of relative energy losses per unit time $E^{-1}dE/dt$ as function of energy (curve 1). Also plotted is the derivative $db_0(E)/dE$, where $b_0(E) = dE/dt$ (Fig. 1b). This quantity is needed for calculation of differential energy spectrum (see section III). In Fig. 1 we plot for comparison the energy losses as calculated by Berezinsky and Grigorieva 1988 [19] (dashed curve 2). The difference in energy losses due to pion production is very small, not exceeding 5% in the energy region relevant for comparison with experimental data ($E \leq 10^{21}$ eV). The difference with energy losses due to pair production is larger and reaches maximal value 15%. The results of calculations by Stanev et al [18] are shown by black squares. These authors have performed the detailed calculations for both aforementioned processes, though their approach is somewhat different from ours, especially for photopion process. Our energy losses are practically indistinguish-

able from [18] for pair production and low energy pion production, and differ by 15-20% for pion production at highest energies (see Fig. 1). Stanev et al claimed that energy losses due to pair production is underestimated by Berezhinsky and Grigorieva [19] by 30-40%. Comparison of *data files* of Stanev et al and Berezhinsky and Grigorieva (see also Fig.1) shows that this difference is significantly less. Most probably, Stanev et al scanned inaccurately the data from the journal version of the paper [19].

III. UNIFORM DISTRIBUTION OF UHECR SOURCES AND GZK CUTOFF

The GZK cutoff is a model-dependent feature of the spectrum, e.g. the GZK cutoff for a single source depends on the distance to the source. A common convention is that the GZK cutoff is defined for diffuse flux from the sources uniformly distributed over the universe. In this case one can give two definitions of the GZK cutoff. In the first one the cutoff is determined as the energy, $E_{GZK} \approx 3 \times 10^{19} \text{ eV}$, where the steep increase in the energy losses starts (see Fig. 1). The GZK cutoff starts at this energy. The corresponding pathlength of a proton is $R_{GZK} \approx (E^{-1}dE/dt)^{-1} \approx 1.3 \cdot 10^3 \text{ Mpc}$. The advantage of this definition of the cutoff energy is independence on spectrum index, but this energy is too low to judge about presence or absence of the cutoff in the measured spectrum. More practical definition is $E_{1/2}$, where the flux with cutoff becomes lower by factor 2 than power-law extrapolation. This definition is convenient to use for the integral spectrum, which is better approximated by power-law function, than the differential one. In Fig.2 the function $E^{(\gamma-1)}J(> E)$, where $J(> E)$ is calculated integral diffuse spectrum, is plotted as function of energy. Note, that $\gamma > \gamma_g$ is an effective index of power-law approximation of the spectrum modified by energy losses. For wide range of generation indices $2.1 \leq \gamma_g \leq 2.7$ the cutoff energy is the same, $E_{1/2} \approx 5.3 \cdot 10^{19} \text{ eV}$. The corresponding proton pathlength is $R_{1/2} \approx 800 \text{ Mpc}$.

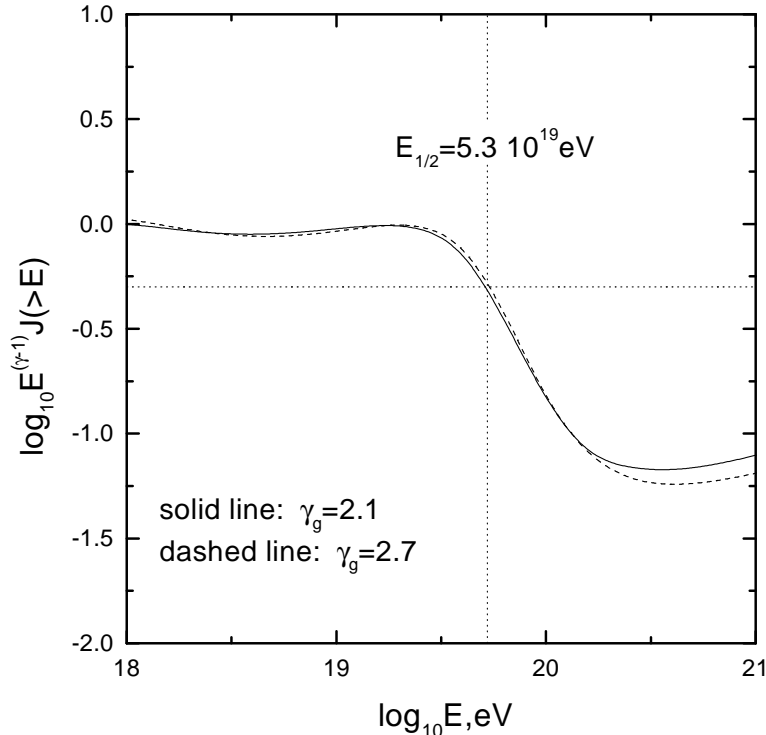


FIG. 2. *Integral UHECR spectra with indices of generation spectra $\gamma_g = 2.1$ and $\gamma_g = 2.7$ (solid and dashed line, respectively). The vertical dotted line shows the energy $E_{1/2}$, where the calculated flux becomes two times lower than power-law extrapolation.*

Using energy losses given in Section 2, we calculated the diffuse spectra for the model when sources are distributed uniformly in the universe. We followed the method of calculation suggested in Ref. [19]. We use two assumptions for uniform distribution of the sources: (i) with evolution of the sources described by factor $(1+z)^m$ in comoving frame [1], and (ii) without evolution. The power-law generation spectrum with index γ_g was assumed. We made different assumptions about maximum energy in the generation spectrum, namely $E_{\max} = 3 \cdot 10^{20}$ eV, $E_{\max} = 1 \cdot 10^{21}$ eV, and $E_{\max} = \infty$. Varying parameters γ_g and m we fit the AGASA and Akeno data [22].

The fit of UHECR data with help of evolving sources was made in the past (e.g. see Ref. [21] and [1]). The widely used fit for the AGASA data with $\gamma_g = 2.3$ and with assumed mixed composition of galactic and extragalactic UHECR was found by Yoshida and Teshima

[22]. Recently Scully and Stecker [23] made calculations similar to that above for UHECR produced by GRBs.

We calculate spectra using the formalism of Ref. [19]:

$$J_p(E) = (\gamma_g - 2) \frac{c}{4\pi} \frac{\mathcal{L}_0}{H_0} E^{-\gamma_g} \int_0^{z_{max}} dz_g (1 + z_g)^{m-5/2} \lambda^{-\gamma_g}(E, z_g) \frac{dE_g(z_g)}{dE}, \quad (4)$$

where z_g is a redshift at generation and $E_g(z_g)$ is energy of a proton at generation, if at present ($z = 0$) its energy is E : $E_g(z_g) = \lambda(E, z_g)E$ and $\lambda(E, z_g)$ is calculated numerically using energy losses dE/dt accounted for their time evolution; $\mathcal{L}_0 = n_0 L_p$ is CR emissivity at $z = 0$ (n_0 and L_p are space density of the sources and their CR luminosity, respectively). As the general case we assume cosmological evolution of the sources given by $\mathcal{L}(z) = \mathcal{L}_0(1+z)^m$, where the absence of evolution corresponds to $m = 0$. All energies in Eq.(4) are given in GeV and luminosities in GeV/s. Dilation of energy interval is given by [19] (see also Appendix B):

$$\frac{dE_g(z_g)}{dE} = (1 + z_g) \exp \left[\int_0^{z_g} \frac{dz}{H_0} (1 + z)^{1/2} \left(\frac{db_0(E')}{dE'} \right)_{E'=(1+z)E_g(z_g)} \right], \quad (5)$$

where $b_0(E) = dE/dt$ is energy loss due to interaction with CMBR photons at $z = 0$ (adiabatic energy loss due to redshift must not be included!). Derivative $db_0(E)/dE$ at $z = 0$ is given in Fig.(1b).

For particles with energies $E \gtrsim 1 \times 10^{17}$ eV the maximum redshift for evolution of CR sources z_{max} is not important if it is larger than 4. Integration over large z gives small contribution when the generation energy $E_g(E, z)$ reaches the value $E_{eq}(z_m)$, at which energy losses due to pair production and redshift are equal. Then the maximum redshift $z_m(E)$ of the epochs contributing to the flux of protons with energy E is determined by equation $(1 + z_m)E = E_{eq}(z_m)$. For energies $E < 1 \times 10^{17}$ eV the maximum redshift of the source evolution z_{max} might be important. In these cases we fix it as $z_{max} = 4$.

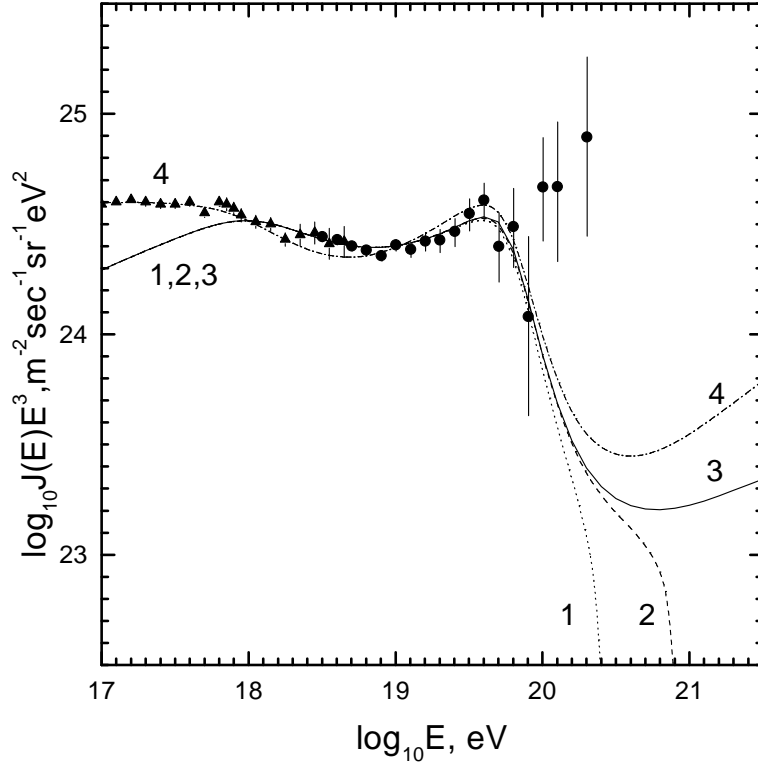


FIG. 3. *UHECR spectrum as observed in Akeno (triangles) and AGASA (filled circles) experiments. The curves show the predicted differential spectra for the uniform distribution of sources with or without evolution. The case without evolution ($m = 0$, $\gamma_g = 2.7$) is given by curves (1),(2),(3) for maximum generation energy $E_{max} = 3 \cdot 10^{20}$ eV, $1 \cdot 10^{21}$ eV and ∞ , respectively. The dashed curve 4 describes the evolutionary model with $m = 4$, $\gamma_g = 2.45$ and $E_{max} = \infty$.*

We can fit the Akeno-AGASA data in both cases, with and without evolution. The spectra without evolution, $m = 0$ can fit the data starting from relatively high energy $E \geq 1 \cdot 10^{18}$ eV. The fit needs $\gamma_g = 2.7$. The curves 1, 2 and 3 in Fig.3 show the spectra with different E_{max} equal to $3 \cdot 10^{20}$ eV, $1 \cdot 10^{21}$ eV and ∞ , respectively. The fit without evolution (curves 1, 2, 3) needs $\mathcal{L}_0 = 4.7 \cdot 10^{51}$ erg/Mpc³yr, while the fit for evolutionary case (curve 4) needs $\mathcal{L}_0 = 1.3 \cdot 10^{49}$ erg/Mpc³yr. The difference between these two emissivities is caused mainly by flatter generation spectrum in the evolutionary case.

The required emissivities can be compared with most powerful local emissivity given by Seyfert galaxies $\mathcal{L}_{Sy} = n_{Sy} L_{Sy}$. Using the space density of Seyfert galaxies $n_{Sy} \sim 10^{-77}$ cm⁻³

and the luminosity $L_{Sy} \sim 10^{44}$ erg/s one obtains $\mathcal{L}_{Sy} \sim 1 \cdot 10^{48}$ erg/Mpc³yr, which is almost 4 orders of magnitude less than CR emissivity needed in no-evolutionary case and one order of magnitude less than one in the evolutionary case.

As Fig.3 shows the models with uniform distribution of the sources are excluded by absence of GZK cutoff in the observations. They give a good fit to the lower energy data. This fit needs large γ_g and thus too large energy output of the sources, nL . It is possible to overcome this difficulty using an assumption that production spectrum is flat at low energies and has a steepening at some high energy E_c . Assuming, for example, that spectrum is $\propto E^{-2}$ at low energy, and $\propto E^{-2.7}$ at $E \geq E_c = 1 \times 10^9$ GeV, one obtains the required CR emissivity (see Section V) $\mathcal{L} = 3.7 \times 10^{46}$ erg/Mpc³yr, i.e. less than observed total emissivity due to the Seyfert galaxies. A plausible assumption is that the population of UHECR sources is comprised by galaxies with moderate activity of AGN, which at higher luminosities are linked to Seyfert galaxies and BL Lacertae. There were recently found the observational indications that the latter galaxies could be the sources of observed UHECR [24]. If such sources had large local overdensity, the GZK cutoff would be less noticeable. We shall study this possibility in the next Section.

IV. LOCAL OVERDENSITY OF UHECR SOURCES

Local overdensity of UHECR sources makes the GZK cutoff less sharp or eliminates it [1]. Clustering of galaxies is a gravitational property, which is determined by mass and not by internal activity of an object. The galaxies of the same masses with active galactic nuclei or without them, with burst of star formation or in quiet phase, are clustering in the same way. Therefore the optical catalogues give a reasonable indication to expected clustering of UHECR sources.

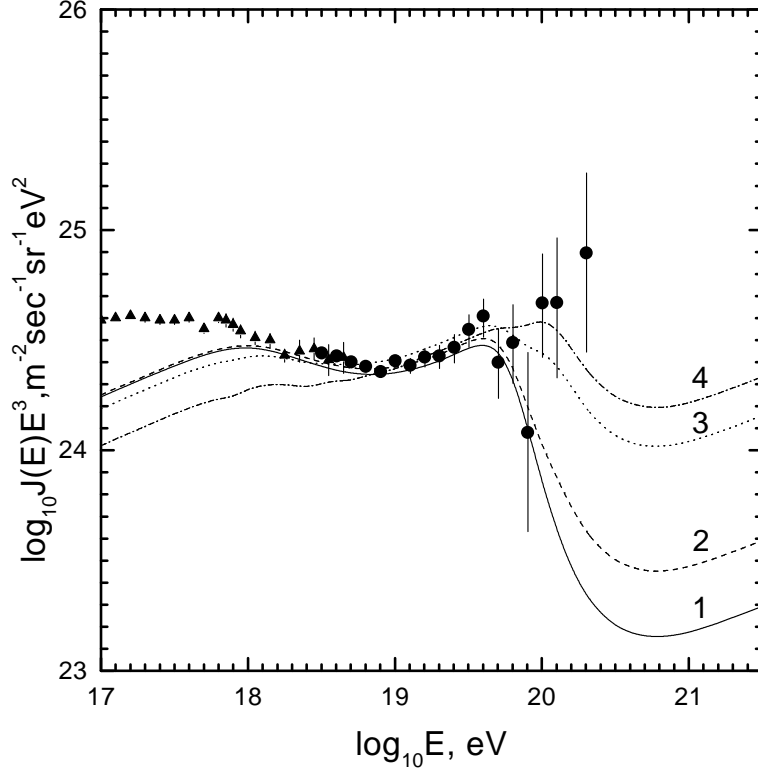


FIG. 4. *The effect of source overdensity on UHECR spectra for $R_{overd} = 30$ Mpc and different overdensity ratios $n/n_0 = 1, 2, 10, 30$ (curves 1, 2, 3 and 4, respectively).*

The nearby structure that can affect the GZK cutoff is Local Supercluster (LS) of galaxies, which has a form of ellipsoid with semi-axes 20 and 30 Mpc. The LS overdensity of galaxies is estimated by factor ~ 2 (see [25] and references therein). Such overdensity does not solve the problem of GZK cutoff [7,8]. We shall calculate here UHECR spectra for different local overdensities n/n_0 , where n_0 is mean extragalactic density of UHECR sources. We use the various sizes of overdensity region R_{overd} , equal to 10, 20 and 30 Mpc. The results of our calculations are presented in Fig.4 for $\gamma_g = 2.7$, $m = 0$ and for four values of overdensity n/n_0 equal to 1, 2, 10 and 30, assuming the size of overdensity region 30 Mpc (the results for $R_{overd} = 20$ Mpc are not much different). From Fig.4 one can see that overdensity $n/n_0 \gtrsim 10$ is needed to reconcile well the calculations with observational data.

V. UHECR FROM GRB

In GRBs the protons can be accelerated to Ultra High Energies [26,27]. The strong indication that UHECR can be produced by GRBs, the authors of Ref. [26,27,9] see in the equal emissivity \mathcal{E} in GRBs and UHECRs. Scully and Stecker [23] argue that in fact the energy output in cosmic rays is higher than in GRBs. We shall analyse here the problem of energy output combined with the spectrum shape.

For energetically most favourable CR generation spectrum dE/E^2 , advocated in [26,27], the diffuse spectrum of UHECR can be found as

$$J_p(E) = \frac{c}{4\pi} \frac{1}{\ln \frac{E_{max}}{E_{min}}} \frac{\mathcal{L}_0}{H_0} E^{-2} \int_0^{z_{max}} dz_g (1+z_g)^{m-5/2} \lambda^{-2}(E, z_g) \frac{dE_g}{dE}. \quad (6)$$

The calculated spectra for non-evolutionary case $m = 0$ and for evolution of GRB sources with $m = 4$ are displayed in Fig.5 by curves 1 and 3, respectively. The required CR emissivity is $\mathcal{L}_0 = 2.0 \cdot 10^{45}$ erg/Mpc³yr for both cases. It is two orders of magnitude larger than that observed in GRBs [28] $\mathcal{E}_{GRB} = 1 \cdot 10^{43}$ erg/Mpc³yr.

Apart from the problem of too large energy output, these models do not fit the observed spectrum shape and predict the standard GZK cutoff. To obtain the agreement with spectrum shape one can use an artificial E^{-2} spectrum with steepening at energy E_c .

At energy $E > E_c$ the generation spectrum of a source is

$$Q_g(E_g, z) = \frac{L_p(z) E_c^{\gamma_g-2}}{\ln \frac{E_c}{E_{min}} + \frac{1}{\gamma_g-2}} E_g^{-\gamma_g}, \quad (7)$$

while at $E < E_c$ this spectrum is assumed to have $1/E^2$ shape. It is easy to verify that this spectrum is correctly normalized to the luminosity L_p . The diffuse spectrum can be readily calculated at $E \geq E_c$ as

$$J_p(E) = \frac{cH_0^{-1}}{4\pi} \mathcal{L}_0 \frac{E_c^{\gamma_g-2} E^{-\gamma_g}}{\ln \frac{E_c}{E_{min}} + \frac{1}{\gamma_g-2}} \int_0^{z_{max}} dz_g (1+z_g)^{m-5/2} \lambda^{-\gamma_g}(E, z_g) \frac{dE_g}{dE}. \quad (8)$$

The fluxes given by Eq.(8) are displayed in Fig.5 by curves 2 and 4 for cases $m = 0$ and $m = 4$, respectively. These spectra agree well with the Akeno-AGASA observations at energies lower

than the GZK cutoff, but require higher emissivity, $\mathcal{L}_0 = 3.7 \cdot 10^{46}$ erg/Mpc³yr ($m = 0$ case, curve 2) and $\mathcal{L}_0 = 3.1 \cdot 10^{46}$ erg/Mpc³yr ($m = 4$ case, curve 4).

We conclude thus that UHECR from GRBs exhibit the standard GZK cutoff and require CR emissivity 2 – 3 orders of magnitude higher than that observed in GRBs. Our conclusions agree with that of Ref. [23].

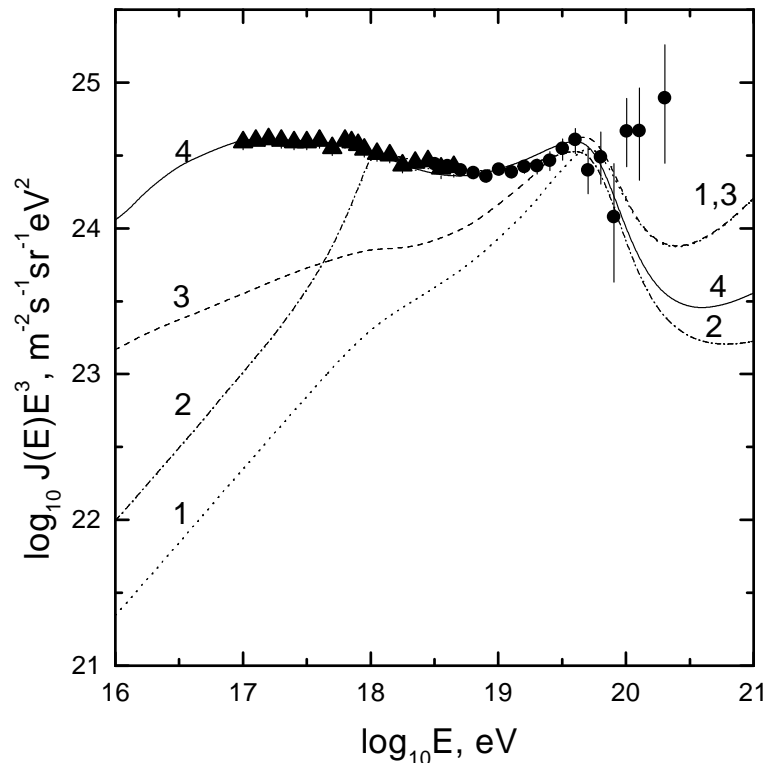


FIG. 5. *UHECR spectra from GRBs for E^{-2} generation spectrum (curve 1 for non-evolutionary $m = 0$ case and curve 3 for evolutionary $m = 4$ case) and for E^{-2} spectrum with steepening (curve 2 for $m = 0$, $E_c = 1 \cdot 10^9$ GeV, $\gamma_g = 2.7$, and curve 4 for $m = 4$, $E_c = 1 \cdot 10^8$ GeV, $\gamma_g = 2.45$)*

VI. CONCLUSIONS

We have performed accurate calculations of energy losses of UHE protons due to electron-positron pair production and pion production in collisions with microwave photons. The diffuse spectra of UHE protons have been calculated for uniform distribution of the sources

in the universe for different maximum energies of the generation spectrum. The generation spectrum with index $\gamma_g = 2.7$ provides a good fit for energy range $1 \cdot 10^{18} - 8 \cdot 10^{19}$ eV in case of absence of evolution. For the case of evolution the good fit is given by $m = 4$ and $\gamma_g = 2.45$ in the energy range $1 \cdot 10^{17} - 8 \cdot 10^{19}$ eV.

Local overdensity of UHECR sources, e.g. in Local Supercluster, can reconcile the weak GZK cutoff with UHECR data only if overdensity is larger than 10. The existing astronomical data favour much smaller overdensity, of order of 2.

The excellent fit of observational data in energy range $1 \cdot 10^{17} - 8 \cdot 10^{19}$ eV by astrophysical spectrum is rather impressive. It requires too high local CR emissivity $\mathcal{L}_0 \sim 1 \cdot 10^{49}$ erg/Mpc³yr (in case of an evolutionary model), but this emissivity can be drastically reduced down to $3 \cdot 10^{46}$ erg/Mpc³yr by assumption of E^{-2} spectrum with steepening at $E_c = 1 \cdot 10^8$ GeV. Normal galaxies with weak AGN (*quasi-seyfert*s) meet this energy requirement. The local overdensity of these galaxies could ameliorate the GZK problem, but required overdensity, $n/n_0 \geq 10$, is larger than that observed $n/n_0 \approx 2$.

UHECR from GRBs have a standard GZK cutoff. The predicted E^{-2} generation spectrum gives bad fit to the observed spectrum at energy lower than GZK cutoff. In case the generation spectrum is modified to give a reasonable fit, the required CR emissivity exceeds that observed in GRBs by three orders of magnitude.

ACKNOWLEDGEMENTS

We are grateful to Todor Stanev who provided us with data file of energy losses calculated in Ref. [18]. We thank M.Teshima for sending us the AGASA data for zenith angles $\theta \leq 45^\circ$ which were used in these calculations (the data for $\theta \leq 60^\circ$ are still preliminary).

The work was partially supported by INTAS through grant INTAS 99-1065 and by Russian Foundation for Basic Research grant 00-15-96632.

APPENDIX A: CALCULATIONS OF ENERGY LOSSES

Pair production energy loss of ultrahigh-energy protons in low-energy photon gas, e.g. *CMBR*,

$$p + \gamma_{CMBR} \rightarrow p + e^+ + e^- \tag{A1}$$

has been previously discussed in many papers. The differential cross-section for this process in the first Born approximation was originally calculated in 1934 by Bethe and Heitler [29] and Racah [30]. In 1948 Feenberg and Primakoff [31] obtained the pair production energy loss rate using the extreme relativistic approximation for the differential cross-section. And in 1970 the accurate calculation was performed by Blumenthal [10]. Later some analytical approximations to differential cross-sections were applied to this problem in Ref. [32].

All authors neglected the recoil energy of proton putting $m_p \rightarrow \infty$, the effect being suppressed by a factor of $m_e/m_p \approx 5 \times 10^{-4}$.

In spite of the fact that all calculations actually used the same Blumenthal approach, there are noticeable discrepancies in the results of different authors; they were clearly demonstrated in Fig. 1b of the Ref. [18].

To clarify the situation we recalculated the pair production energy loss of high-energy proton in the low-energy photon gas. In contrast to Ref. [10] we use the first Born approximation approach of Ref. [11] taking into account the finite proton mass. The exact non-relativistic threshold formula with corrections to different Coulomb interactions of electron and positron with the proton (see e.g. Ref. [12]) was used. No series expansions of $\sigma(E_\gamma)$ were involved in our calculations.

Our strategy was to calculate the average energy transfer $x = E'_p/E_p$, where E_p and E'_p are the incident and final proton energies respectively, in the laboratory system by performing the direct fourfold integration of the exact matrix element over the phase space. It should be noted, that direct numerical integration, especially at high energies, is difficult in this

case because of forward-backward spikes in the electron-positron angular distributions. To overcome this problem, we performed two integrations over polar and azimuth angles in the e^+e^- subsystem analytically. This was facilitated by using of the *MATHEMATICA 4* code. The residual two integrations over energy and scattering angle in the initial $p\gamma$ subsystem were carried out numerically. We calculate simultaneously the total cross-section for pair production. The accuracy of our calculations was thus controlled by comparison of calculated total cross-section with the well-known Bethe-Heitler cross-section.

The average fraction of proton energy lost in one collision with a photon is plotted in Fig. 6 as a function of the photon energy in the proton rest system.

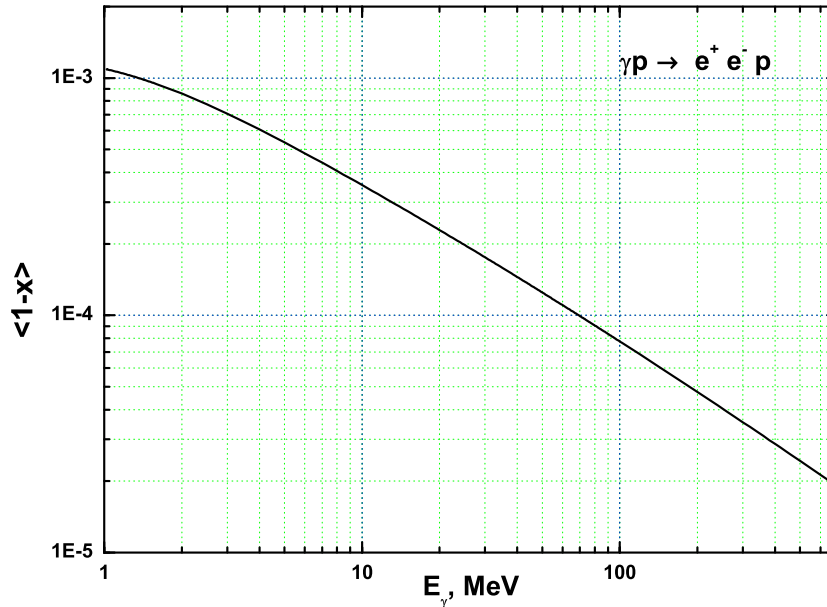


FIG. 6. The average fraction of the incident proton energy E_p carried away by e^+e^- pair as a function of the photon energy E_γ in the proton rest system.

The product of this fraction and the total cross-section for pair production is shown in Fig. 7. This function should be integrated over the photon spectrum to obtain the average energy loss due to pair production in the photon gas with this spectrum.

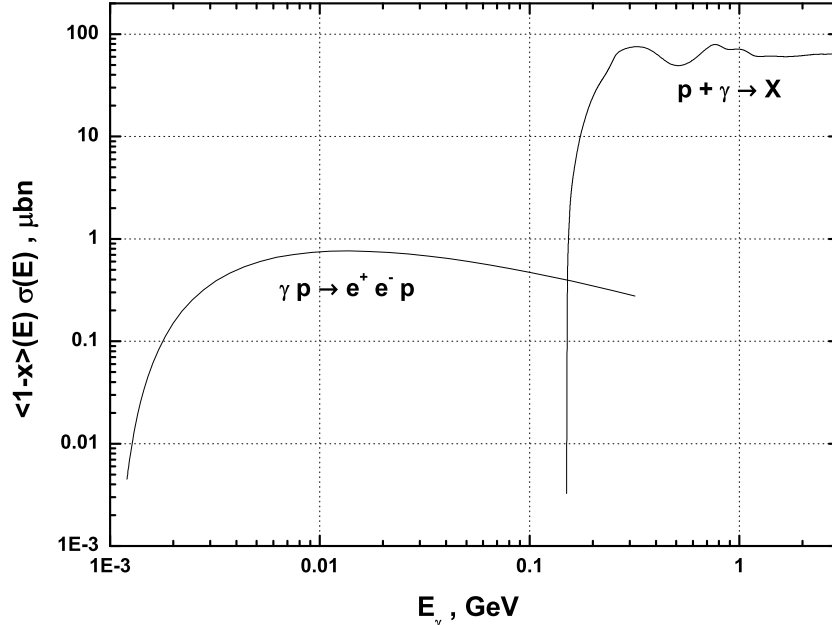


FIG. 7. The product of fraction of energy lost, $\langle 1-x \rangle$, and the cross-section for pair production, $\gamma p \rightarrow e^+ e^- p$, or photopion production $p + \gamma \rightarrow X$ as function of photon energy in the proton rest system E_γ .

The comparison of our calculations with Ref. [18] shows the negligible difference (see Fig. 1).

APPENDIX B: CONNECTION BETWEEN ENERGY INTERVALS AT EPOCHS OF PRODUCTION AND OBSERVATION

If we consider the protons with energy E in the interval dE at the epoch with redshift $z = 0$, what will be the corresponding interval of generation dE_g at epoch z , when energy of a proton was $E_g(z)$? The connection between these two intervals is given by Eq.(36) of Ref. [19]. Here we shall confirm this formula using a different, more simple derivation. Note, that intermediate formulae (40) and (41) used for derivation of final Eq.(36) in Ref. [19] have a misprint: the correct power of $(1+z)$ term there is 3, not 2.

Regarding the energy losses of a proton on CMBR, dE/dt and $(1/E)dE/dt$, at arbitrary

epoch with redshift z , we shall use the following notation

$$b(E, z) = \left(\frac{dE}{dt} \right)_{\text{CMBR}}, \quad \beta(E, z) = \left(\frac{1}{E} \frac{dE}{dt} \right)_{\text{CMBR}}. \quad (\text{B1})$$

As it is readily seen from Eq.(2), the energy losses at arbitrary epoch z can be found as

$$\beta(E, z) = (1+z)^3 \beta_0((1+z)E), \quad (\text{B2})$$

where notation $b_0(E)$ and $\beta_0(E)$ are used here and henceforth for energy losses at $z = 0$.

The energy loss due to redshift at the epoch z is given by

$$\left(\frac{1}{E} \frac{dE}{dt} \right)_{\text{r-sh}} = H_0(1+z)^{3/2}. \quad (\text{B3})$$

The energy of a particle at epoch z ,

$$E_g(z) = E + \int_t^{t_0} dt \left[\left(\frac{dE}{dt} \right)_{\text{r-sh}} + \left(\frac{dE}{dt} \right)_{\text{CMBR}} \right], \quad (\text{B4})$$

can be easily rearranged as

$$E_g(z) = E + \int_0^z \frac{dz'}{1+z'} E_g(z') + \frac{1}{H_0} \int_0^z \frac{dz'}{(1+z')^{1/2}} b_0((1+z')E_g(z')), \quad (\text{B5})$$

with help of Eq.(B2) and expression $dt = dz/H_0(1+z)^{5/2}$ for time interval.

Differentiating Eq.(B5) over E , one finds for energy interval dilation $y(z) \equiv dE_g(z)/dE$:

$$y(z) = 1 + \int_0^z \frac{dz'}{1+z'} y(z') + \frac{1}{H_0} \int_0^z dz' (1+z')^{1/2} y(z') \left(\frac{db_0(E')}{dE'} \right)_{E'=(1+z')E_g(z')}. \quad (\text{B6})$$

Corresponding differential equation is

$$\frac{1}{y(z)} \frac{dy(z)}{dz} = \frac{1}{1+z} + \frac{1}{H_0} (1+z)^{1/2} \left(\frac{db_0(E')}{dE'} \right)_{E'=(1+z)E_g(z)}. \quad (\text{B7})$$

The solution of Eq.(B7) is

$$y(z) \equiv \frac{dE_g(z)}{dE} = (1+z) \exp \left[\frac{1}{H_0} \int_0^z dz' (1+z')^{1/2} \left(\frac{db_0(E')}{dE'} \right)_{E'=(1+z')E_g(z')} \right], \quad (\text{B8})$$

where $E_g(z)$ is an energy at epoch z . Eq.(B8) coincides with Eq.(36) from Ref. [19].

REFERENCES

- [1] V.S. Berezhinskii, S. V. Bulanov, V. A. Dogiel, V. L. Ginzburg, and V.S. Ptuskin, *Astrophysics of Cosmic Rays*, North-Holland, 1990.
- [2] K.Greisen, *Phys. Rev. Lett.*, **16** (1966) 748;
G. T. Zatsepin and V. A. Kuzmin, *Pisma Zh. Experim. Theor. Phys.*, **4** (1966) 114.
- [3] M.Nagano and A. A. Watson, *Rev. of Mod. Phys.* **72** (2000) 689.
- [4] J.Wdowczyk and A. Wolfendale, *Nature* **281** (1980) 356;
M. Giler, J. Wdowczyk and A. Wolfendale, *J. Phys. G* **6** (1980) 1561.
- [5] V.S.Berezhinsky, S. I. Grigorieva and V. A. Dogiel, *Astron. Astroph.* **232** (1990) 582.
- [6] E-J Ahn, G. Medina-Tanco, P. L. Biermann and T. Stanev, *Nucl. Phys. (Proc. Suppl.)* **87** (2000) 417.
- [7] V.S.Berezhinsky and S. I. Grigorieva, *Proc. of 16th Int. Cosmic Ray Conf. (Kyoto)*, **2**, (1979) 81.
- [8] M.Blanton, P. Blasi and A. Olinto, *Astrop. Phys.* **15** (2001) 275.
- [9] E.Waxman, *Nuclear Physics B (Proc. Suppl.)* **87** (2000) 345.
- [10] G.R.Blumenthal, *Phys. Rev.* **D1** (1970) 1596.
- [11] R. A. Berg and C. N. Linder, *Nucl. Phys.* **26** (1961) 259.
- [12] V.B.Berestetskii, E. M. Lifshits and L. P. Pitaevskii, *Quantum Electrodynamics* **4** Nauka, Moscow 1980.
- [13] V.Berezhinsky and A. Gazizov, *Phys. Rev.* **D47** (1993) 4206.
- [14] A.Z.Gazizov, *Proc. of the 4th Annual Seminar NPC'S'95, ed't.'s V. Kuvshinov and G. Krylov*, Minsk, Belarus, **6** (1996) 59.

- [15] E.Gabathuler, Proc. of the 6th Int. Symp. on Electron and Photon Interactions at High Energies, North-Holland Publishing Company (1974) 299.
- [16] D.Menze, W. Pfeil and R. Wilke, ZAED compilation of Pion Photoproduction Data, University of Bonn, 1977; G. Wolf and P. Söding, Electromagnetic Interactions of hadrons, Plenum Press, New York **2** (1978) 1; H. M. Fisher, Proc. of the 6th Int. Symp. on Electron and Photon Interactions at High Energies, North-Holland Publishing Company (1974) 77.
- [17] H.Meyer, Proc. of the 6th Int. Symp. on Electron and Photon Interactions at High Energies, North-Holland Publishing Company (1974) 175; F.Brasse, *ibid* 257; K. C. Moffeit et al., Phys. Rev. **D5** (1972) 1603.
- [18] T.Stanev, R. Engel, A. Muecke, R. J. Protheroe and J. P. Rachen, Phys. Rev. **D62** (2000) 093005.
- [19] V.S.Berezinsky and S. I. Grigorieva, Astron. Astroph. **199** (1988) 1.
- [20] M.Teshima, private communication, December 2001. To sew the data of AGASA and Akeno we reduced the energies of AGASA by 10%, as recommended in Ref. [3].
- [21] V.S.Berezinsky and S. I. Grigorieva, Sov. Astron. Lett. **9** (1983) 309.
- [22] S.Yoshida and M. Teshima, Progr. Theor. Phys. **89** (1993) 833.
- [23] S.T.Scully and F. W. Stecker, Astrop.Phys. **14** (2000) 207.
- [24] P.G.Tinyakov and I.I.Tkachev, astro-ph/0102476.
- [25] P.J.E. Peebles, Principles of Physical Cosmology, Princeton University Press, 1993.
- [26] M.Vietri, Ap. J **453** (1995) 883.
- [27] E.Waxman, Phys. Rev. Lett. **75** (1995) 386.

- [28] Maarten Schmidt, *Ap. J.* **523** (1999) L117.
- [29] H.Bethe and W.Heitler, *Proc. Roy. Soc. (London)* **A146** (1934) 83.
- [30] G.Racah, *Nuovo Cimento* **11** (1934) 461.
- [31] E.Feenbeg and H.Primakoff, *Phys.Rev.* **73** (1948) 449 .
- [32] M.Chodorowski, A.A.Zdziarski and M.Sikora, *Astrophys.J.* **400** (1992) 181.